sciendo

Int. J. Appl. Math. Comput. Sci., 2018, Vol. 28, No. 4, 661–677
DOI: 10.2478/amcs-2018-0051

amcs

INTERCONNECTION AND DAMPING ASSIGNMENT PASSIVITY–BASED CONTROL OF AN UNDERACTUATED 2–DOF GYROSCOPE

GUSTAVO CORDERO [a], VÍCTOR SANTIBÁÑEZ [a,*], ALEJANDRO DZUL [a], JESÚS SANDOVAL [b]

[a] Division of Graduate Studies and Research
National Institute of Technology of Mexico/Laguna Institute of Technology
Blvd. Revolución and Cuauhtemoc S/N, 27000 Torreón, Mexico
e-mail: gustavo.cordero.hdz@gmail.com,
vsantiba@itlalaguna.edu.mx,dzul@faraday.itlalaguna.edu.mx

[b] Division of Graduate Studies and Research
National Institute of Technology of Mexico/La Paz Institute of Technology
Blvd. Forjadores de BCS No. 4720, Apdo. Postal 43-B, 23080 La Paz, Mexico
e-mail: jsandoval@itlp.edu.mx

In this paper we present interconnection and damping assignment passivity-based control (IDA-PBC) applied to a 2 degrees of freedom (DOFs) underactuated gyroscope. First, the equations of motion of the complete system (3-DOF) are presented in both Lagrangian and Hamiltonian formalisms. Moreover, the conditions to reduce the system from a 3-DOF to a 2-DOF gyroscope, by using Routh's equations of motion, are shown. Next, the solutions of the partial differential equations involved in getting the proper controller are presented using a reduction method to handle them as ordinary differential equations. Besides, since the gyroscope has no potential energy, it presents the inconvenience that neither the desired potential energy function nor the desired Hamiltonian function has an isolated minimum, both being only positive semidefinite functions; however, by focusing on an open-loop nonholonomic constraint, it is possible to get the Hamiltonian of the closed-loop system as a positive definite function. Then, the Lyapunov direct method is used, in order to assure stability. Finally, by invoking LaSalle's theorem, we arrive at the asymptotic stability of the desired equilibrium point. Experiments with an underactuated gyroscopic mechanical system show the effectiveness of the proposed scheme.

Keywords: gyroscope device, gyroscopic forces, cyclic coordinates, generalized momenta, Routh's equations, IDA-PBC.

1. Introduction

Interconnection and damping assignment passivity-based control (IDA-PBC) is a control design methodology based on a total energy shaping approach. A desired dynamic in the closed-loop system is proposed as a control objective, where, usually, a set of partial differential equations (PDEs) needs to be solved. Since the introduction of IDA-PBC by Ortega *et al*. (2002), several theoretical extensions and practical applications have been reported in the literature. Acosta *et al*. (2005) presented a strategy for PDEs to become ordinary differential equations (ODEs) under certain conditions, while Kotyczka and Lohmann (2009) present a parametrization of IDA-PBC by assignment of local linear dynamics. Gómez-Estern and van der Schaft (2004) as well as Sandoval *et al*. (2011) presented some extensions of the IDA-PBC to handle physical damping. Chang (2014) proposes a manner to introduce quadratic gyroscopic forces instead of the skew-symmetric interconnection submatrix allowing a reduction of PDEs. Meanwhile, Donaire *et al*. (2016) present robust IDA-PBC for underactuated mechanical systems subject to matched disturbances adding an outer-loop controller (e.g., a nonlinear PID).

On the other hand, the IDA-PBC method, employed for position regulation for some underactuated mechanical systems, has been reported in the literature; some examples include an inertia wheel pendulum and a ball and beam (Ortega *et al*., 2002), a pendulum on a cart and a vertical takeoff and landing aircraft (VTOL), an acrobot robot (Mahindrakar *et al*., 2006), or following a

*Corresponding author

pendubot robot (Sandoval *et al*., 2008), among others. It is worth remarking that, in recent years, some authors have invented a way to shape the energy of mechanical systems without solving PDEs (Donaire *et al*., 2015), and even they were able to propose PID passivity-based control to reach global stabilization of underactuated mechanical systems (Romero *et al*., 2017).

Underactuated mechanical systems have fewer independent control inputs than degrees of freedom to be controlled, which means that the external generalized forces are not able to command instantaneous accelerations in all directions in the configuration space (Fantoni and Lozano, 2002). Spacecraft (e.g., Aguilar-Ibanez, 2016), underwater vehicles, mobile robots, surface vessels, and many other systems have this characteristic. A detailed survey of underactuated mechanical systems, classification, and some control methods can be found in the work of Liu and Yu (2013). Several controller design methodologies for the stabilization of underactuated mechanical systems usually validate their results with 2-DOF mechanisms because of their simplicity, as remarked by She *et al*. (2012), and they have been focused on the regulation problem (Moreno-Valenzuela and Aguilar-Avelar, 2018), especially in the so-called benchmark systems: the cart pole, TORA system, rotary inverted pendulum, Furuta pendulum and pendubot (e.g., Antonio-Cruz *et al*., 2018), acrobot, ball and beam, etc. Recently, attention has been paid to greater degrees of freedom underactuated mechanical systems; some examples are modern light-weight flexible robots and articulated manipulators with passive joints. Besides, other important types are flexible multibody systems, since their body elasticity generates additional underactuated degrees of freedom (Seifried, 2014). The effect of friction in underactuated multibody systems is also addressed, e.g., by Liu (2018), who deals with discontinuous friction.

The gyroscope is a very special and singular mechanism to be controlled by IDA-PBC, because it has no potential energy function and total energy shaping is challenging. It has symmetries which essentially imply an invariance of the system, often with respect to inertial positioning, yielding *cyclic* coordinates, and, in the absence of external constraints, this invariance implies the existence of inertial nonholonomic constraints, which adopt the form of momentum conservation laws (Ostrowski and Burdick, 1997). Besides, a nonholonomic system could not be asymptotically stabilized at an equilibrium point using a smooth static state feedback law (Bloch *et al*., 1992; Wichlund *et al*., 1995; Jiang, 2010). Furthermore, in general, the absence of potential energy adds an interesting challenge for any controller design methodology to get asymptotical stabilization of any underactuated mechanism (its gravitational field has zero elements corresponding to underactuated dynamics) (Chin *et al*., 2006).

According to the IDA-PBC method, the desired energy function qualifies as a Lyapunov function for the desired equilibrium (Mahindrakar *et al*., 2006); however, this occurs when the mechanical system has potential energy. Nevertheless, when the mechanical system has no potential energy, the IDA-PBC method leads to a desired potential energy function that is not positive definite and, in consequence, does not have an isolated minimum. Therefore, we analyze the desired total energy function to find out if some features of the open-loop system help to build a positive definite function. This is the main motivation of our work since the gyroscope does not present potential energy.

Our contributions in this paper are as follows: (i) reduction of equations of motion from a 3-DOF to a 2-DOF gyroscope by using Routh's process for ignoring coordinates, (ii) detection and interpretation of gyroscopic terms as a generalized potential energy function that also leads to the reinterpretation of generalized momenta, (iii) the application of the IDA-PBC method to a system having no potential energy, (iv) evidence that a nonholonomic constraint, and not the desired potential energy function, helps to assign the desired equilibrium point, (v) the stability proof of the desired equilibrium point of the desired closed-loop system using LaSalle's theorem, and (vi) experimental validation of the effectiveness of the IDA-PBC method applied to an underactuated gyroscopic mechanical system.

Notation. In this paper we use n for the number of degrees of freedom, $I_{n\times n}$ is the identity matrix and $0_{n\times n}$ is the $n \times n$ matrix of zeros, and m is the number of actuated joints. Position and generalized momenta are time-dependent, that is, $q = q(t)$ and $p = p(t)$. We define the differential operator $\nabla_x H := \partial H/\partial x$, where $H : \mathbb{R}^n \to \mathbb{R}$ is a continuous function and $x : \mathbb{R}_+ \to \mathbb{R}^n$ is the state vector. Besides, $(\cdot)^\top$ denotes a transpose, $(\cdot)^{-1}$ denotes an inverse, $(\cdot)^\perp$ denotes a full rank left annihilator of $(\cdot)$, $(\cdot)^*$ refers to a value of $(\cdot)$ at the equilibrium point, $\tilde{(\cdot)}$ denotes an error, $\bar{(\cdot)}$ refers to an auxiliary generalized momentum vector. S_i and C_i with $i \in \{1, 2, 3\}$ are equivalent to $\sin(q_i)$ and $\cos(q_i)$, respectively. Finally, $(\star)_{(\cdot)d}$ is the desired position of $(\star)_{(\cdot)}$, while $(\star)_{(\cdot)}(0)$ is the initial condition of $(\star)_{(\cdot)}$.

2. Preliminaries

2.1. Brief review of the IDA-PBC method for a class of mechanical systems. The IDA-PBC method begins with the total energy function of the underactuated mechanical system in terms of the generalized momenta $p \in \mathbb{R}^n$ and position $q \in \mathbb{R}^n$ using the so-called

Hamiltonian function[1]

$$H(q,p) = \frac{1}{2}p^\top M^{-1}(q)p + V(q), \tag{1}$$

where $M = M^\top > 0 \in \mathbb{R}^{n\times n}$ is the inertia matrix and V is the potential energy function. If we do not consider the system's natural damping (e.g., friction), then the equations of motion in Hamiltonian form can be written as

$$\begin{bmatrix} \dot{q} \\ \dot{p} \end{bmatrix} = \begin{bmatrix} 0_{n\times n} & I_{n\times n} \\ -I_{n\times n} & 0_{n\times n} \end{bmatrix} \begin{bmatrix} \nabla_q H \\ \nabla_p H \end{bmatrix} + \begin{bmatrix} 0 \\ G(q) \end{bmatrix} u, \tag{2}$$

where $G \in \mathbb{R}^{n\times m}$ indicates how the control input $u \in \mathbb{R}^m$ enters the system (the actuator's distribution matrix) and is invertible when the system is fully actuated (G is a square matrix); otherwise, if we have an underactuated mechanism, then G has no inverse and $\text{rank}(G) = m < n$.

Ortega *et al*. (2002) proposed the following desired closed-loop energy function:

$$H_d(q,p) = \frac{1}{2}p^\top M_d^{-1}(q)p + V_d(q), \tag{3}$$

where $M_d = M_d^\top > 0 \in \mathbb{R}^{n\times n}$ and V_d are the desired inertia matrix and potential energy function of the closed-loop system, respectively. Moreover, the desired dynamic in the closed-loop system is proposed with the following structure:

$$\begin{bmatrix} \dot{q} \\ \dot{p} \end{bmatrix} = \begin{bmatrix} 0 & M^{-1}M_d \\ -M_dM^{-1} & J(q,p) - GK_vG^\top \end{bmatrix} \times \begin{bmatrix} \nabla_q H_d \\ \nabla_p H_d \end{bmatrix}, \tag{4}$$

where $J = -J^\top \in \mathbb{R}^{n\times n}$ is a free-parameter matrix and $K_v = K_v^\top > 0$. Besides, we require that V_d have an isolated minimum in q^*, that is,

$$q^* = \arg\min V_d, \tag{5}$$

in order to get an asymptotically stable equilibrium point $(q^*, 0)$ of (4), with Lyapunov function H_d, taking into account that M_d is positive definite at least in a neighborhood of q^*.

By matching $[\dot{q}^\top \;\; \dot{p}^\top]$ from the models (2) and (4) and splitting the terms, we arrive at the following PDEs:

$$G^\perp\{\nabla_q\left(p^\top M^{-1}p\right) - M_dM^{-1}\nabla_q\left(p^\top M_d^{-1}p\right) + 2JM_d^{-1}p\} = \mathbf{0}_{n-m}, \tag{6}$$

$$G^\perp\{\nabla_q V - M_dM^{-1}\nabla_q V_d\} = \mathbf{0}_{n-m}, \tag{7}$$

[1]To simplify the notation, hereafter for all expressions which are functions of q and p we will write explicitly their dependence only the first time they are defined.

where $G^\perp(q) \in \mathbb{R}^{(n-m)\times n}$ is a full rank left annihilator of G, i.e., $G^\perp G = \mathbf{0}_{(n-m)\times m}$ and $\text{rank}(G^\perp) = n - m$. If it is possible to get a solution for M_d and V_d from Eqns. (6) and (7), then IDA-PBC of the system (2) is

$$u = (G^\top G)^{-1}G^\top(\nabla_q H - M_dM^{-1}\nabla_q H_d + JM_d^{-1}p) - K_vG^\top\nabla_p H_d. \tag{8}$$

2.2. Reduction from a PDE to an ODE. By following the procedure used by Acosta *et al*. (2005), we proceed to the reduction of the PDE (6), which is possible since the gyroscope has underactuation degree one, i.e., $m = n-1$, and the matrix M does not depend on the underactuated coordinate. Equation (6) is reduced to the form

$$e_k^\top M^{-1}M_d(G^\perp)^\top\frac{\mathrm{d}M_d}{\mathrm{d}q_k} = -2\mathcal{J}\mathcal{A}^\top, \tag{9}$$

where $e_k \in \mathbb{R}^n$ is a basis vector, k signifies the actuated coordinate,

$$\mathcal{J} \triangleq [\alpha_1 \vdots \alpha_2 \vdots \cdots \vdots \alpha_{no}] \in \mathbb{R}^{n\times n_o}, \tag{10}$$

where $\alpha_i \in \mathbb{R}^n$, $i = 1,\ldots,n_o$, with $n_o \triangleq (n/2)(n-1)$ as a free parameter vector, and

$$\mathcal{A} \triangleq -[W_1(G^\perp)^\top, \ldots, W_{no}(G^\perp)^\top] \in \mathbb{R}^{n\times n_o} \tag{11}$$

is a free matrix, $W_i \in \mathbb{R}^{n\times n}$, with $i = 1,\ldots,n_o$, defined as follows: first, we construct n^2 matrices of dimension $n \times n$ that we denote by $F^{kl} = \{f_{ij}^{kl}\}$, with $k,l \in \{1,2,\ldots,n\}$, according to the rule

$$f_{ij}^{kl} = \begin{cases} 1 & \text{if } \; j > i,\, i = k \text{ and } j = l, \\ 0 & \text{otherwise,} \end{cases} \tag{12}$$

then, we define $W_i = W^{kl} \triangleq F^{kl} - (F^{kl})^\top$. Besides, we are using the fact that

$$\nabla_q\left(p^\top M_d^{-1}p\right) = p^\top\frac{\mathrm{d}}{\mathrm{d}q_k}\left(M_d^{-1}(q_k)\right)pe_k. \tag{13}$$

Note that Eqn. (9) corresponds to Eqn. (18) in the work of Acosta *et al*. (2005).

2.3. Routh's process for ignoring coordinates. Consider a dynamical system with n degrees of freedom specified by n generalized coordinates $q_1, q_2, \ldots, q_n$, with kinetic energy function $\mathcal{K}(q,\dot{q}) = \frac{1}{2}\dot{q}^\top M\dot{q}$, potential energy function $V(q)$ and input control τ, expressed with Euler–Lagrange's equation as

$$\frac{\mathrm{d}}{\mathrm{d}t}\left[\frac{\partial\mathcal{L}(q,\dot{q})}{\partial\dot{q}}\right] - \frac{\partial\mathcal{L}(q,\dot{q})}{\partial q} = \tau \tag{14}$$

with

$$\mathcal{L} = \mathcal{K} - V, \tag{15}$$

or expressed in Hamilton's equations (2), where the generalized momentum is given by

$$p = \frac{\partial \mathcal{L}}{\partial \dot{q}} = M\dot{q}. \tag{16}$$

For the system (14), we have the following definitions and theorems.

Definition 1. (*Cyclic coordinates*) The coordinate q_j, with $j \in \{1, \ldots, n\}$, which does not appear explicitly in the expression for the Lagrangian or the Hamiltonian function, is by definition called *cyclic* or *ignorable*. A change in these coordinates cannot affect the Lagrangian or the Hamiltonian (Rana and Joag, 1991).

Theorem 1. (Rana and Joag, 1991, Ch. 2, Sect. 12) *In the absence of applied external torque τ, the generalized momentum corresponding to any cyclic coordinate is a conserved quantity (it is a constant of motion).*

Proof. Let q_j be a cyclic coordinate. Then, by Definition 1,

$$\frac{\partial \mathcal{L}}{\partial q_j} = 0.$$

Hence, Euler–Lagrange's equation (14) for coordinate q_j reduces to

$$\frac{\mathrm{d}}{\mathrm{d}t}\left[\frac{\partial \mathcal{L}}{\partial \dot{q}_j}\right] = \tau_j \equiv 0.$$

Therefore,

$$p_j = \frac{\partial \mathcal{L}}{\partial \dot{q}_j} = P_j = \text{ constant of motion.} \tag{17}$$

■

If such a conserved quantity (17) is not integrable, then a class of nonholonomic systems is obtained (Reyhanoglu and van de Loo, 2006a).

Definition 2. (*Nonholonomic constraints*) If a system has *nonintegrable* constraints on their velocities, then it has nonholonomic constraints. Meanwhile, holonomic systems are mechanical systems that are subject to constraints that limit their possible configurations; systems with nonholonomic constraints restrict the type of motion but not position (Bloch, 2003). An angular momentum may be viewed as a nonholonomic constraint when it is an invariant of the motion (Bloch *et al.*, 1992).

Definition 3. (*Routh's equations of motion*) Let the system have k-cyclic coordinates $q_1, q_2, \ldots, q_k$ $(k < n)$. Then, the dynamical system has $(n - k)$ degrees of freedom. Clearly, the generalized momentum corresponding to the cyclic coordinate would be (17). Define a new function $\mathcal{R}$ as

$$\mathcal{R}(q, \dot{q}) = \mathcal{L} - \sum_{j=1}^{k} P_j \dot{q}_j, \tag{18}$$

which is called the Routhian function and $\mathcal{L}$ is the Lagrangian function defined in (15). The new equations of motion ignoring the cyclic coordinates can be obtained as

$$\frac{\mathrm{d}}{\mathrm{d}t}\left[\frac{\partial \mathcal{R}(q, \dot{q})}{\partial \dot{q}_i}\right] - \frac{\partial \mathcal{R}(q, \dot{q})}{\partial q_i} = \tau_i \tag{19}$$

for $i = k + 1, k + 2. \ldots, n$ (Layek, 2015). This shows that $\mathcal{R}$ behaves as a Lagrangian $\mathcal{L}$ of the new dynamical system (19) having $(n - k)$ degrees of freedom.

Property 1. Note that if the original system (14) has symmetries, then, after lowering the number of degrees of freedom, gyroscopic forces appear in the new dynamical system (19). They also occur as a result of a transformation towards a rotating reference frame (Kozlov, 1996).

2.4. Gyroscopic forces. Gyroscopic forces occur if the system contains a rotating body and the configuration is expressed relative to this body or if the system has cyclic coordinates (Greenwood, 1977). An important characteristic of gyroscopic terms is that a coupling of the motions, in two or more coordinates, is always involved (Kang *et al.*, 2003).

Definition 4. (*Gyroscopic forces*)

(a) They are often used to designate terms in the kinetic energy $\varphi^\top(q)\dot{q}$ that are linear in the velocity components, where $\varphi : \mathbb{R}^k \to \mathbb{R}^k$ (Ferraz-Mello, 2007).

(b) The gyroscopic forces $\Gamma(q)\dot{q}$, where $\Gamma : \mathbb{R}^n \to \mathbb{R}^{n\times n}$, are forces that conserve energy since they are perpendicular to the velocity of the mechanism, implying that they do not realize any work (Sabattini *et al.*, 2017). Formally, a force

$$f_{\text{gyro}}(q, \dot{q}) = \Gamma(q)\dot{q}, \tag{20}$$

where $\Gamma = \{\gamma_{ij}(q)\}$ is a skew-symmetric matrix (that is, $\Gamma^\top = -\Gamma$) is called gyroscopic if $f_{\text{gyro}}^\top \dot{q} = 0$ (Kang *et al.*, 2003).

An easy way to identify gyroscopic forces, in the equations of motion, is to observe the terms of the form $\gamma_{ij}\dot{q}_j$, where the gyroscopic coefficients γ_{ij} are skew symmetric, i.e., $\gamma_{ij} = -\gamma_{ji}$. This means, as stated before, that those gyroscopic forces do not work in the equations of motion (Nagata and Namachchivaya, 2006). Note that gyroscopic energy terms $\varphi^\top(q)\dot{q}$ yield gyroscopic forces $\Gamma(q)\dot{q}$.

Property 2. The gyroscopic force is always perpendicular to the velocity of the mechanism, doing no work; this property guarantees that they do not modify the convergence characteristics of the desired control laws (Sabattini *et al*., 2017).

Property 3. Gyroscopic forces can never destabilize a stable conservative system, but they can possibly stabilize an unstable conservative one (Seyranian *et al*., 1995).

Definition 5. (*Generalized potential energy*) The generalized potential energy function $W(q,\dot{q})$ can, in most cases, be conveniently represented by the sum of an ordinary potential energy function and a term coming from the kinetic energy function that is linear in $\dot{q}$ (Rana and Joag, 1991) (which in turn yield gyroscopic forces (20) of antisymmetric nature in the equations of motion); that is,

$$W(q,\dot{q}) = V(q) + \varphi^{\top}(q)\dot{q}. \tag{21}$$

This class of potential energy function is velocity dependent. In this way, $\mathcal{L} = \mathcal{K} - W$, and thus the momentum yields

$$p = \frac{\partial \mathcal{L}}{\partial \dot{q}} = \frac{\partial(\mathcal{K}-W)}{\partial \dot{q}} = M\dot{q} - \frac{\partial W}{\partial \dot{q}} \tag{22}$$

while the corresponding Hamiltonian is given by (Ferraz-Mello, 2007)

$$H = \frac{1}{2}p^{\top}M^{-1}(q)p + Y(q,p), \tag{23}$$

where

$$Y(q,p) = W(q,p) - \frac{1}{2}\left(\frac{\partial W(q,\dot{q})}{\partial \dot{q}}\right)^{\top} M^{-1}\frac{\partial W(q,\dot{q})}{\partial \dot{q}}. \tag{24}$$

3. Gyroscope and a dynamic model

3.1. Gyroscope. The gyroscope is a device with a spinning disc where, based on the conservation of angular momentum, while it rotates, the orientation of its axis is unaffected by rotation of the mounting. Due to this fact, it is used for keeping and/or measuring the orientation of a body in space. Usually, the disc is mounted on a Cardan suspension, which is often a set of three gimbals, one mounted on the other with orthogonal pivot axes. The testbed used in this work is the Gyroscope platform system from Quanser® , and it is shown in Fig. 1 (for more information about this gyroscope we recommend the lecture of Quanser (2009)). It consists of a 3-DOF rotor D assembled on the innermost gimbal C which is in turn placed inside an outer gimbal B which in turn is put on a rectangular frame A. The plant is equipped with four DC motors to provide spin torque and four encoders to provide position feedback; signals (torque and position) are transmitted to the structure's base due to a slip ring design. Any of these gimbals can be fixed in order to have different configurations and to reduce the degrees of freedom. The mass center of all bodies and gimbals axes are at the center of the disc.

3.2. Dynamic model. In Appendix A we develop in detail the kinetic and potential energy functions of a 3-DOF gyroscope. In order to obtain Lagrange's equations of motion, we calculate first the Lagrangian, taking into account that the gyroscope potential energy function $V(q) = 0$. Then the Lagrangian is also the kinetic energy function, i.e.,

$$\begin{aligned}\mathcal{L}(q,\dot{q}) &= \mathcal{K} - V = \mathcal{K} \\ &= \frac{1}{2}I_{Dxx}\dot{q}_1^2 + \frac{1}{2}J_3\dot{q}_2^2 \\ &\quad - I_{Dxx}S_2\dot{q}_1\dot{q}_3 + \frac{1}{2}(J_2 + J_1S_2^2)\dot{q}_3^2,\end{aligned} \tag{25}$$

where q_1 is the motion of the disk D, q_2 the motion of the body C and q_3 the motion of body B, while I_{Dxx}, J_1, J_2, and J_3 are inertia parameters (see Table 1) and $S_2 := \sin(q_2)$. By applying Lagrange's equations of motion (14), we get the 3-DOF gyroscope dynamic model:

$$I_{Dxx}[\ddot{q}_1 - C_2\dot{q}_2\dot{q}_3 - S_2\ddot{q}_3] = \tau_1, \tag{26}$$

$$J_3\ddot{q}_2 + I_{Dxx}C_2\dot{q}_1\dot{q}_3 - J_1S_2C_2\dot{q}_3^2 = \tau_2, \tag{27}$$

$$\begin{aligned}&(J_2 + J_1S_2^2)\ddot{q}_3 + 2J_1S_2C_2\dot{q}_2\dot{q}_3 \\ &\quad -I_{Dxx}[S_2\ddot{q}_1 + C_2\dot{q}_1\dot{q}_2] = \tau_3,\end{aligned} \tag{28}$$

where τ_1, τ_2 and τ_3 are the external torques applied (similar results for the dynamic model (26)–(28) are

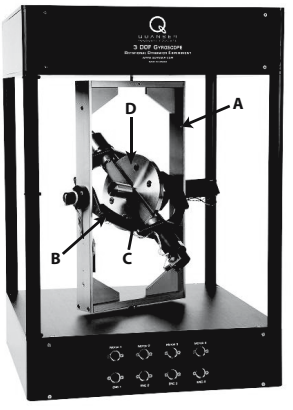

Fig. 1. Gyroscope by Quanser and the body nomenclature.

presented by Reyhanoglu and van de Loo (2006a; 2006b)). From Eqns. (26)–(28) we can easily extract the inertia matrix of the 3-DOF gyroscope,

$$M = \begin{bmatrix} I_{Dxx} & 0 & -I_{Dxx}S_2 \\ 0 & J_3 & 0 \\ -I_{Dxx}S_2 & 0 & J_2 + J_1 S_2^2 \end{bmatrix}, \tag{29}$$

and knowing that the conjugate momentum p_j of the system (also known as a canonical momentum or generalized momentum), with $j \in \{1,2,3\}$, is $p = \partial \mathcal{L}/\partial \dot{q} = M\dot{q}$, we get

$$p_1 = I_{Dxx}\dot{q}_1 - I_{Dxx}S_2\dot{q}_3, \tag{30}$$

$$p_2 = J_3\dot{q}_2, \tag{31}$$

$$p_3 = -I_{Dxx}S_2\dot{q}_1 + (J_2 + J_1 S_2^2)\dot{q}_3. \tag{32}$$

Having the inertia matrix M and assuming that no potential energy is present, we can use Eqn. (1) to obtain the Hamiltonian function

$$H(q,p) = \frac{1}{2}\left[\frac{p_1^2}{I_{Dxx}} + \frac{(p_3 + p_1 S_2)^2}{J_2 + J_a S_2^2} + \frac{p_2^2}{J_3}\right], \tag{33}$$

where $J_a = J_1 - I_{Dxx}$, and thus, by using (2), Hamilton's equations of motion of the 3-DOF gyroscope are

$$\begin{bmatrix} \dot{q}_1 \\ \dot{q}_2 \\ \dot{q}_3 \\ \dot{p}_1 \\ \dot{p}_2 \\ \\ \dot{p}_3 \end{bmatrix} = \begin{bmatrix} \frac{(J_2 + J_1 S_2^2)\frac{p_1}{I_{Dxx}} + p_3 S_2}{J_2 + J_a S_2^2} \\ \frac{p_2}{J_3} \\ \frac{p_3 + p_1 S_2}{J_2 + J_a S_2^2} \\ \tau_1 \\ \frac{J_a S_2 C_2 (p_3 + p_1 S_2)^2}{(J_2 + J_a S_2^2)^2} \\ -\frac{p_1 C_2 (p_3 + p_1 S_2)}{(J_2 + J_a S_2^2)} + \tau_2 \\ \tau_3 \end{bmatrix}, \tag{34}$$

considering that the open loop system is fully actuated.

3.3. Reducing equations of motion. If we analyze Eqns. (25) and (33), we can observe that there exist two *cyclic* coordinates, q_1 and q_3 (see Definition 1). Besides, by considering $\tau_1 = 0$, since we are assuming that we have reached a constant speed of the disk and no torque is needed to keep this speed (because the friction of the disk is neglected), the conjugate momentum p_1 of (30) is a constant (let $p_1 = P_1$ be this constant). This allows us to reduce one degree of freedom since we can express $\dot{q}_1$ in terms of a constant P_1 in the equations of motion (27) and (28). Also, this assumption implies, from (30), that the disk speed remains constant when no movement of q_2 is detected.

In addition, since we want to work with an underactuated gyroscope, by turning the motor off, $\tau_3 = 0$; this causes that the conjugate momentum p_3 of (32) is constant (P_3), i.e., it can be reduced another degree of freedom since $\dot{q}_3$ can be expressed in terms of a constant P_3 in the equation of motion (27). However, we will not reduce this degree of freedom in order to be able to assign the closed-loop equilibrium point.

An alternative way to get a reduction in the degree of freedom related to the cyclic coordinate q_1 is to apply Routh's process for ignoring cyclic coordinates (Layek, 2015) as declared in Definition 3. That is,

$$\mathcal{R} = \mathcal{L} - P_1\dot{q}_1, \tag{35}$$

$$\dot{q}_1 = \frac{P_1 + I_{Dxx}S_2\dot{q}_3}{I_{Dxx}}. \tag{36}$$

If we substitute (25) and (36) in (35), we obtain the Routhian of the new system as

$$\mathcal{R} = -\frac{1}{2}\frac{{P_1}^2}{I_{Dxx}} + \frac{1}{2}J_3\dot{q}_2^2 + \frac{1}{2}(J_2 + J_a S_2^2)\dot{q}_3^2 - P_1 S_2\dot{q}_3, \tag{37}$$

and by substituting (37) in (19) we get the new Lagrange-equivalent equations of motion of the dynamical system corresponding to a 2-DOF gyroscope,

$$J_3\ddot{q}_2 + P_1 C_2\dot{q}_3 - J_a S_2 C_2\dot{q}_3^2 = \tau_2, \tag{38}$$

$$(J_2 + J_a S_2^2)\ddot{q}_3 + 2J_a S_2 C_2\dot{q}_2\dot{q}_3 - P_1 C_2\dot{q}_2 = 0. \tag{39}$$

The set of equations (38) and (39) correspond to those developed by Cannon (1967). Another simple way to obtain (38) and (39) could be by substituting (36) in (32) to get

$$p_3 = -S_2 P_1 + (J_2 + J_a S_2^2)\dot{q}_3. \tag{40}$$

Then, by substituting (36) in (27), we get (38), and differentiating (40) with respect to time, we get (39), i.e., the same reduced equations of motion.

Now, after reducing the equation of motion, and by virtue of Property 1, it is expected to have gyroscopic terms. From (37) it can be observed, by using Definition 4(a), that it has an energy gyroscopic term $\varphi_3\dot{q}_3 = P_1 S_2\dot{q}_3$ because it is linear in the velocity component (Ferraz-Mello, 2007). From Definition 5, this term can be introduced in the generalized potential energy $W(q,\dot{q}) = V(q) + \varphi^\top(q)\dot{q}$ as

$$W(q,\dot{q}) = V + \varphi_3\dot{q}_3 = P_1 S_2\dot{q}_3. \tag{41}$$

In addition, if we analyze (38) and (39), by using Definition 4(b) we realize that they have gyroscopic forces of the form $f_{\text{gyro}}(q,\dot{q}) = \Gamma(q)\dot{q}$ as

$$\Gamma(q)\dot{q} = \begin{bmatrix} 0 & P_1 C_2 \\ -P_1 C_2 & 0 \end{bmatrix}\begin{bmatrix} \dot{q}_2 \\ \dot{q}_3 \end{bmatrix}. \tag{42}$$

Now, using (38) and (39), we can get the new inertia matrix for the 2-DOF gyroscope,

$$M = \begin{bmatrix} J_3 & 0 \\ 0 & J_2 + J_a S_2^2 \end{bmatrix}. \tag{43}$$

Note that for the reduced system (38)–(39) with generalized potential energy W (gyroscopic energy terms) this produces gyroscopic forces in the equations of motion. The definition of the conjugate momentum (16) is no longer valid. Instead, we have the new definition of the the conjugate momentum (22) and thus, by substituting (41) and (43) into (22), we obtain

$$p_2 = J_3 \dot{q}_2, \tag{44}$$

$$p_3 = -P_1 S_2 + (J_2 + J_a S_2^2)\dot{q}_3. \tag{45}$$

If we take (45), by solving it for $\dot{q}_3$ and substituting the result in (41), we have W in dependence on (q, p) as

$$W(q,p) = \frac{P_1 S_2 (p_3 + P_1 S_2)}{J_2 + J_a S_2^2}. \tag{46}$$

Finally, we can get the Hamiltonian function for the reduced system, using $p = [p_2 \;\; p_3]^\top$, (41), (46), M^{-1} from (43) and applying (23) with (24), so we have

$$H(q,p) = \frac{1}{2}\left[\frac{p_2^2}{J_3} + \frac{(p_3 + P_1 S_2)^2}{J_2 + J_a S_2^2}\right]. \tag{47}$$

Another way to get (47) is using an auxiliary vector

$$\bar{p} = \left[p + \frac{\partial W}{\partial \dot{q}}\right] \tag{48}$$

and the following identity with the same structure of (1):

$$H = \frac{1}{2}\left[p + \frac{\partial W}{\partial \dot{q}}\right]^\top M^{-1}\left[p + \frac{\partial W}{\partial \dot{q}}\right] + V \tag{49}$$

which, after substituting $p = [p_2 \;\; p_3]^\top$, (41) and M^{-1} from (43), produces

$$H = \frac{1}{2}\begin{bmatrix} p_2 \\ p_3 + P_1 S_2 \end{bmatrix}^\top \begin{bmatrix} \frac{1}{J_3} & 0 \\ 0 & \frac{1}{J_2 + J_a S_2^2} \end{bmatrix} \cdot \begin{bmatrix} p_2 \\ p_3 + P_1 S_2 \end{bmatrix}, \tag{50}$$

which in turn yields (47). This identity between (23) and (49) is demonstrated in Appendix B. In this way, the open-loop system, in the Hamiltonian formalism, can be rewritten as

$$\begin{bmatrix} \dot{q}_2 \\ \dot{q}_3 \\ \dot{p}_2 \\ \dot{p}_3 \end{bmatrix} = \begin{bmatrix} \frac{p_2}{J_3} \\ \frac{p_3 + P_1 S_2}{J_2 + J_a S_2^2} \\ \frac{J_a S_2 C_2 (p_3 + P_1 S_2)^2}{(J_2 + J_a S_2^2)^2} \\ -\frac{P_1 C_2 (p_3 + P_1 S_2)}{(J_2 + J_a S_2^2)} + \tau_2 \\ 0 \end{bmatrix}, \tag{51}$$

and it can be noticed that the equations in (51) correspond to those proposed in (34), with $\dot{q}_1$ and $\dot{p}_1$ removed and p_1 substituted by P_1, validating thereby our model (51).

It is important to underscore from Eqn. (51) that we have a nonholonomic constraint related to $\dot{q}_3$ (see Definition 2), which is nonintegrable in nature and will restrict the type of motion of the associated variables. This nonholonomic constraint is observed at the equilibrium when $\dot{q}_3 = 0$. To this end, first we explore the open-loop equilibria of the system by making the left-hand side of (51) zero and assuming that no external forces are actuating over the system. Then we find that $p_3 + P_1 S_2 = 0$. However, as mentioned before, p_3 must be constant ($p_3 = P_3$) since it is related to a cyclic coordinate q_3 and it is underactuated, so the term S_2 must be constant for all $t \geq 0$, and its value necessarily comes from an initial condition $q_2(0)$ that produces the constant $S_2 = S_2(0) = \sin(q_2(0))$. In consequence, at the equilibrium we have

$$P_3 = -P_1 S_2(0), \tag{52}$$

and since

$$P_3 + P_1 S_2 = 0, \quad \forall\, t \geq 0,$$

which implies

$$S_2 = -\frac{P_3}{P_1} = \frac{P_1 S_2(0)}{P_1} = S_2(0),$$

we have

$$q_2 = q_2(0), \quad \forall\, t \geq 0. \tag{53}$$

Meanwhile, as q_3 is a *cyclic* coordinate, it can take any initial value $q_3(0)$. Thereby, there exists an infinite number of equilibriums

$$[q_2, q_3, p_2, p_3]^\top = [q_2(0), q_3(0), 0, P_3]^\top \in \mathbb{R}^4. \tag{54}$$

By Definition 2 and by virtue of (52), we have that, at the equilibrium, when $\dot{q}_3 = 0$, q_2 is restricted to be $q_2(0)$. This is essentially the nonholonomic constraint. This means that, at the equilibrium, q_2 could never be arbitrary (imposed by the user), i.e., q_2 could never be other than $q_2(0)$, neither in the closed-loop system.

4. IDA-PBC of the 2-DOF gyroscope

4.1. Control objective. Given the open-loop Hamiltonian system (51), associated with the Hamiltonian function (47), the control aim is to find a control law u such that we get a closed-loop Hamiltonian system given by (4) associated with the desired Hamiltonian function (3) in such a way that the following position objective is achieved:

$$\lim_{t \to \infty} \begin{bmatrix} q_2(t) \\ q_3(t) \end{bmatrix} = \begin{bmatrix} q_2(0) \\ q_{3d} \end{bmatrix}. \tag{55}$$

4.2. Kinetic energy function. In order to get IDA-PBC for the 2-DOF gyroscope, we follow Eqn. (9), forming

$$\mathcal{J} \triangleq \begin{bmatrix} \alpha_a(q) \\ \alpha_b(q) \end{bmatrix}, \quad \mathcal{A} \triangleq \begin{bmatrix} -1 \\ 0 \end{bmatrix}, \tag{56}$$

using the fact that $-2\mathcal{J}\mathcal{A}^\top = -[\mathcal{J}\mathcal{A}^\top + \mathcal{A}\mathcal{J}^\top]$, we get

$$-2\mathcal{J}\mathcal{A}^\top = \begin{bmatrix} 2\alpha_a & \alpha_b \\ \alpha_b & 0 \end{bmatrix}. \tag{57}$$

Finally, using the equivalence presented by (Sandoval *et al.*, 2008)

$$\Lambda(q) = M_d M^{-1} = \begin{bmatrix} \lambda_1(q) & \lambda_2(q) \\ \lambda_3(q) & \lambda_4(q) \end{bmatrix}, \tag{58}$$

Eqn. (9) becomes

$$e_2^\top \Lambda^\top (G^\perp)^\top \frac{\mathrm{d}M_d}{\mathrm{d}q_2} = \begin{bmatrix} 2\alpha_a & \alpha_b \\ \alpha_b & 0 \end{bmatrix}. \tag{59}$$

Now, by using (58) and solving for M_d, we get $M_d = \Lambda M$. Substituting (58) and (43) in this result, we have

$$M_d = \begin{bmatrix} \lambda_1 J_3 & \lambda_2(J_2 + J_a S_2^2) \\ \lambda_3 J_3 & \lambda_4(J_2 + J_a S_2^2) \end{bmatrix}. \tag{60}$$

For the gyroscope, $G = [1\ 0]^\top$ and the base vector is $e_k = e_2 = [1\ 0]^\top$. Substituting (58) and (60) into (59), we obtain the following equations:

$$\lambda_3 \frac{\mathrm{d}}{\mathrm{d}q_2}\lambda_1 J_3 - 2\alpha_a = 0, \tag{61}$$

$$\lambda_3 \frac{\mathrm{d}}{\mathrm{d}q_2}\lambda_2(J_2 + J_a S_2^2) - \alpha_b = 0, \tag{62}$$

$$\lambda_3 \frac{\mathrm{d}}{\mathrm{d}q_2}\lambda_3 J_3 - \alpha_b = 0, \tag{63}$$

$$\lambda_3 \frac{\mathrm{d}}{\mathrm{d}q_2}\lambda_4(J_2 + J_a S_2^2) = 0. \tag{64}$$

Equations (61)–(64) are no longer PDEs. They became ODEs. By starting with (64), we get the following values for $\lambda_i, i \in \{1, 2, 3, 4\}$:

$$\lambda_4 = \frac{k_4}{J_2 + J_a S_2^2}, \tag{65}$$

$$\lambda_3 = k_3, \tag{66}$$

$$\lambda_2 = \frac{\lambda_3 J_3}{(J_2 + J_a S_2^2)}, \tag{67}$$

$$\lambda_1 = k_1. \tag{68}$$

Substituting (65)–(68) into (60), we obtain the desired inertia matrix

$$M_d = \begin{bmatrix} k_1 J_3 & k_3 J_3 \\ k_3 J_3 & k_4 \end{bmatrix}, \tag{69}$$

taking into account that $\lambda_3 J_3 = \lambda_2(J_2 + J_a S_2^2)$ and $k_1 k_4 > k_3^2 J_3$ to ensure that $M_d = M_d^\top > 0$. Meanwhile k_1, k_3 and k_4 are arbitrary constants, and α_a and α_b were set to zero.

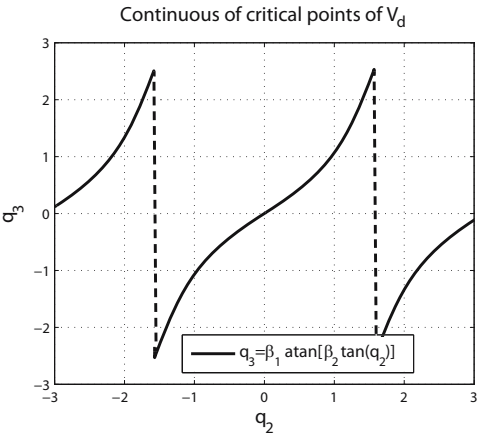

Fig. 2. Infinite number of critical points of V_d for some arbitrary β_1 and β_2.

4.3. Desired potential energy function. In order to get the desired potential energy function, being aware that there is no potential energy for the gyroscope in the open-loop system, i.e., $\nabla_q V = 0$, and by substituting in (7) the left annihilator matrix $G^\perp$, (58), (65) and (66), we arrive at the following PDE:

$$k_3 \nabla_{q2} V_d + \frac{k_4}{J_2 + J_a S_2^2} \nabla_{q3} V_d = 0, \tag{70}$$

which can be solved analytically or by using a mathematical program like Maple© whose solution is $V_d(q_2, q_3) = F(s(q_2, q_3))$, with s as follows:

$$s = q_3 - q_{3d} - \beta_1 \mathrm{atan}[\beta_2 \tan(q_2 - q_2(0))], \tag{71}$$

where

$$\beta_1 = \frac{k_4}{k_3\sqrt{J_2(J_a + J_2)}},$$

$$\beta_2 = \frac{(J_a + J_2)}{\sqrt{J_2(J_a + J_2)}}.$$

We added the terms q_{3d} and $q_2(0)$ to set the desired equilibrium point. To assure the positivity of V_d, we propose, for simplicity, the following function:

$$V_d = F(s) = \frac{1}{2} K_p s^2. \tag{72}$$

In order to obtain the critical points of (72), we make $\nabla_q V_d = 0$, getting

$$q_2 \in \mathbb{R}, \tag{73a}$$

$$q_3 = q_{3d} + \beta_1 \mathrm{atan}[\beta_2 \tan(q_2 - q_2(0))]. \tag{73b}$$

Notice that there exist an infinite number of critic points, one for each $q_2 \in \mathbb{R}$. This behavior can be seen in Fig. 2. In particular, for $q_2 = q_2(0)$, we have the critical

point $(q_2, q_3) = (q_2(0), q_{3d})$. However, V_d is a positive semidefinite function with respect to q_2 and q_3. From the IDA-PBC method, it is supposed that the function V_d has an isolated minimum in q^*, in order to make the closed-loop Hamiltonian function positive definite at least locally; but, V_d has an infinite number of critical points due to the lack of a contributive term related to the open-loop potential energy. This leads us to review other considerations on the stability analysis.

Once we have obtained M_d and V_d, we can compute the desired Hamiltonian function H_d, by using (3) and the auxiliary vector of generalized momentums, as proposed in (48), so we get

$$H_d = \frac{1}{2}\begin{bmatrix} p_2 \\ p_3 + P_1 S_2 \end{bmatrix}^\top \begin{bmatrix} k_1 J_3 & k_3 J_3 \\ k_3 J_3 & k_4 \end{bmatrix}^{-1} \cdot \begin{bmatrix} p_2 \\ p_3 + P_1 S_2 \end{bmatrix} + \frac{1}{2} K_p s^2, \tag{74}$$

which, with some algebraic manipulations, yields

$$H_d = \frac{1}{2}\left[\frac{k_1(p_3 + P_1 S_2)^2 - 2k_3 p_2(p_3 + P_1 S_2) + \frac{p_2^2 k_4}{J_3}}{k_1 k_4 - J_3 k_3^2}\right] + \frac{1}{2} K_p s^2. \tag{75}$$

From (74), the minima of H_d are at $p_2 = 0$, $p_3 + P_1 S_2 = 0$ and $s = q_3 - q_{3d} - \beta_1 \text{atan}[\beta_2 \tan(q_2 - q_2(0))] = 0$, then we have $p_3 = -P_1 S_2$. However, by virtue of (52), we have $p_3 = P_3 = -P_1 \sin(q_2(0))$. Thus $-P_1 \sin(q_2(0)) = -P_1 \sin(q_2)$. This implies $q_2 = q_2(0)$, which, when substituted in $s = 0$, yields $q_3 = q_{3d}$. In this way, the function (75) has a unique minimum at $[q_2 \ q_3 \ p_2 \ p_3]^\top = [q_2(0) \ q_{3d} \ 0 \ P_3]^\top$ and it is a positive definite function by virtue of the nonholonomic constraint (45).

Remark 1. Since the function V_d in (72) is only positive semidefinite, so is (75). But due to the conservation of the generalized momentum $p_3 = P_3$ that imposes a nonholonomic constraint on q_2 of the form $p_3 = P_3 = -P_1 S_2(0)$, for all $t \geq 0$, this implies that H_d has a unique minimum occurring if and only if $q_2 = q_2(0)$, such that H_d in (75) is a positive definite function by virtue of (52) and, as a result, it qualifies as a Lyapunov function for the stability analysis.

Substituting (47) and (75), with $J = 0$, M and M_d as in (43) and (69), respectively, in Eqn. (8), we find the following IDA-PBC for the 2-DOF gyroscope:

$$u = \tau_2 = u_1 + u_2 + u_3 - u_4, \tag{76}$$

where

$$u_1(q,p) = -\frac{J_a S_2 C_2 (p_3 + P_1 S_2)^2}{(J_2 + J_a S_2^2)^2}, \tag{77}$$

$$u_2(q,p) = \frac{P_1 C_2 (p_3 + P_1 S_2)}{J_2 + J_a S_2^2}, \tag{78}$$

$$u_3(q) = \frac{K_p s (k_1 k_4 - k_3^2 J_3)}{k_3 (J_2 + J_a S_2^2)}, \tag{79}$$

$$u_4(q,p) = K_v \left[\frac{\frac{k_4 p_2}{J_3} - k_3 (p_3 + P_1 S_2)}{k_1 k_4 - k_3^2 J_3}\right]. \tag{80}$$

Notice that u_1 and u_2 are terms to cancel the open-loop dynamics (51). A block diagram of the IDA-PBC (76) applied to the 2-DOF gyroscope dynamics (51) is shown in Fig. 3. Finally, we are able to get the closed-loop dynamics, by substituting M, M_d, and H_d into (4), to produce

$$\begin{bmatrix} \dot{q}_2 \\ \dot{q}_3 \\ \dot{p}_2 \\ \dot{p}_3 \end{bmatrix} = \begin{bmatrix} \frac{p_2}{J_3} \\ \frac{p_3 + P_1 S_2}{(J_2 + J a S_2^2)} \\ u_3 - u_4 \\ 0 \end{bmatrix}. \tag{81}$$

We can explore the equilibrium point of the closed-loop system by making the left-hand side of (81) zero. By observing that the first two equations, $\dot{q}_2 = 0$ and $\dot{q}_3 = 0$ lead to $p_2 = 0$ and $p_3 + P_1 S_2 = 0$, which in turn, by using (52), yields $q_2 = q_2(0)$. Now, by exploring the third equation related to $\dot{p}_2 = 0$, with $u_4 = 0$ (since $p_2 = 0$ and $p_3 + P_1 S_2 = 0$), we arrive at $s = 0$. By substituting this result into (71), and knowing that $q_2 = q_2(0)$, we get $q_3 = q_{3d}$, concluding that the unique equilibrium point of (81) is

$$[q_2, q_3, p_2, p_3]^\top = [q_2(0), q_{3d}, 0, P_3]^\top \in \mathbb{R}^4. \tag{82}$$

5. Stability analysis

Previously, we have proven that H_d in (75) is a positive definite function and, consequently, we can apply

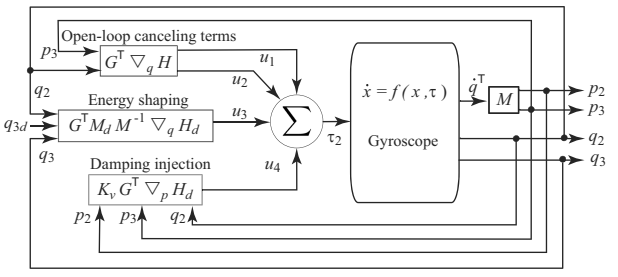

Fig. 3. Block diagram of the IDA-PBC (76) applied to a 2-DOF gyroscope.

Lyapunov's direct method to prove the stability of the equilibrium point (82). Now, we have

$$\begin{aligned}\dot{H}_d &= (\nabla_q H_d)^\top \dot{q} + (\nabla_p H_d)^\top \dot{p} \\ &= -(\nabla_p H_d)^\top G K_v G^\top \nabla_p H_d,\end{aligned}$$

which yields

$$\dot{H}_d = -K_v \left[\frac{\frac{k_4 p_2}{J_3} - k_3(p_3 + P_1 S_2)}{k_1 k_4 - k_3^2 J_3} \right]^2 \leq 0, \qquad (83)$$

which is a negative semidefinite function. This means that the desired equilibrium point (82) is stable. Now, we invoke LaSalle's Theorem from (Kelly *et al*., 2005, Theorem 2.7, pp. 49) in order to analyze the asymptotic stability of the equilibrium point (82). By examining Eqn. (83), in accordance to Kelly *et al*. (2005), the set Ω is

$$\begin{aligned}\Omega &= \{x \in \mathbb{R}^4 : \dot{H}_d(x) = 0\} \\ &= \{x = [q^\top \ p^\top]^\top \in \mathbb{R}^4 : \dot{H}_d(x) = 0\} \\ &= \{x = [q^\top \ p^\top]^\top \in \mathbb{R}^4 : \\ &\quad \frac{k_4 p_2}{J_3} - k_3(p_3 + P_1 S_2) = 0\}. \end{aligned} \qquad (84)$$

Then $\dot{H}_d \equiv 0$ when

$$\frac{k_4 p_2}{J_3} - k_3(p_3 + P_1 S_2) \equiv 0. \qquad (85)$$

If we substitute the value of p_2 in terms of $\dot{q}_2$ from (81), and the value of p_3 from (52) into (85), we get

$$k_4 \frac{\mathrm{d}q_2(t)}{\mathrm{d}t} \equiv k_3 P_1 [\sin(q_2(t)) - \sin(q_2(0))]. \qquad (86)$$

Equation (86) is a nonlinear ODE with initial conditions $q_2(0)$, whose unique solution (cf. Appendix C) is

$$q_2(t) \equiv q_2(0). \qquad (87)$$

Also, it implies that $\dot{q}_2 \equiv 0$ and thus

$$p_2 \equiv 0, \qquad (88)$$

which, in turn, yields $\dot{p}_2 \equiv 0$. If we substitute $\dot{p}_2 \equiv 0$ into the third equation of (81), knowing that $u_4 = 0$ by Eqn. (85), we have that $s \equiv 0$, which, in turn, using (71) and (87), yields

$$q_3 \equiv q_{3d}. \qquad (89)$$

In this way, we prove that the equilibrium point (82) is the maximum invariant set in Ω. Then, according to LaSalle's theorem (Kelly *et al*., 2005, Theorem 2.7), it is sufficient to guarantee the local asymptotic stability of the equilibrium point.

6. Experimental results

We implemented the controller (76) in the Quanser® gyroscope (Fig. 1). The experimental results were validated using Simulink®, utilizing *Quarc accelerate design, version 2.2.1* as real-time control software which uses 1 [ms] for the sample time. Time derivatives were estimated by using a second order filter (filter dynamics are neglected in this paper). We propose the desired position $q_{3d} = 30°$. The gyroscope parameters have been directly obtained from the manufacturer (Quanser, 2009). They are shown in Table 1. Experimental gains are shown in Table 2 (simulation results are omitted due to space limitations). Furthermore, we built a simple proportional controller of the form $\tau_1 = 0.6(\dot{q}_{1d} - \dot{q}_1)$, to fix the speed of the disc at $\dot{q}_{1d} = 750$ [rpm].

We calculate $P_1 = I_{Dxx}\dot{q}_1 = \frac{2\pi}{60}(750)(0.0027) = 0.212057$ [kg · m^2/s]. In the physical gyroscope, the unused joint (q_4) is manually blocked and its attached motor is switched off. The IDA-PBC is enabled once the desired disc velocity is reached. For comparison purposes, we analyze IDA-PBC versus PD-PD controllers, where the PD-PD controller is a cascade proportional-derivative controller shown in the block diagram in Fig. 4, which is defined as follows:

$$\tau_2 = k_{p1}k_{p2}\tilde{q}_3 - k_{p2}k_{v1}\dot{q}_3 - k_{p2}q_2 - k_{v2}\dot{q}_2, \qquad (90)$$

where $\tilde{q}_3 = q_{3d} - q_3$ is the position error, k_{p1}, k_{p2} are strictly positive and named proportional gains, and k_{v1} and k_{v2} are also strictly positive and named derivative gains shown in Table 2.

To quantify the control performance, we use, for the transient period, the settling time t_s and the percentage of overshoot M_p, and for the steady-state period, the root-mean square average of the tracking error (based on the $\mathcal{L}_2$ norm of the tracking errors $\tilde{q}$) given by

$$\mathcal{L}_2[\tilde{q}] = \sqrt{\frac{1}{T - t_0}\int_{t_0}^{T} \tilde{q}^\top \tilde{q} \, \mathrm{d}t} \qquad (91)$$

where T represents the total experimentation time and t_0 is the initial time of the experiment. The better performance is attained for smaller t_s, M_p and $\mathcal{L}_2$ norm (Santibanez *et al*., 2004).

Figure 5 shows the time evolution of q_2 and q_3 positions, where each vanishes to the desired value with

Table 1. Gyroscopic parameters.

$J_1 = 0.0075$ [kg · m^2]
$J_2 = 0.0225$ [kg · m^2]
$J_3 = 0.0036$ [kg · m^2]
$J_a = 0.0048$ [kg · m^2]
$I_{Dxx} = 0.0027$ [kg · m^2]

Table 2. Experimental gains.

IDA-PBC	PD-PD
$k_1 = 0.30$	$k_{p1} = 50.000$
$k_3 = 0.30$	$k_{v1} = 1.000$
$k_4 = 0.01$	$k_{p2} = 0.025$
$K_p = 1.00$	$k_{v2} = 0.500$
$K_v = 0.05$	

Table 3. Performance indexes.

Controller	t_s (2%)	$\mathcal{L}_2[\tilde{q}]$
IDA-PBC	1.2 [s]	0.1797[°]
PD-PD	1.63 [s]	0.2072[°]

both controllers (76) and (90), respectively. Notice that the proposed IDA-PBC (76) produces a faster response than the PD-PD controller (90) without overshoot (M_p). The $\mathcal{L}_2$ norm criterion, taken for the steady-state period (in our case, we take it from t_s to 2 [s]) gives a good comparative performance index for the errors which are shown in Fig. 7, where the errors vanish, concluding that IDA-PBC exhibits better performance. Table 3 summarizes settling times t_s and norms $\mathcal{L}_2$ for each tested control algorithm, also showing better performance for IDA-PBC. The torque needed to reach the control objective is shown in Fig. 6, where it is clear that IDA-PBC needs a smaller amount of torque to accomplish the control objective (55).

We performed some extra tests to show how K_p from IDA-PBC influences the error convergence rate and how it can be increased. In Fig. 8, it can be noticed that, reducing K_p, the error convergence rate decreases since it takes longer time to reach the setpoint. With $K_p > 1.2$ the convergence rate is increased, but an overshoot is obtained. Furthermore, in order to know the behavior of the system facing disturbances, we carried out a second test adding to the system a physical disturbance applied to q_2 with a duration of 0.89 seconds and 9° of intensity. In Fig. 9, it can be noticed that K_v plays an important role in the recovery time to reach the target again when rejecting disturbances; the higher K_v, the shorter time for the system to recover itself.

7. Conclusions

We have presented the IDA-PBC for a 2-DOF gyroscope system, illustrating a way to reduce equations of motion involving cyclic coordinates and gyroscopic forces. We have shown how to detect gyroscopic terms and interpret them as a generalized potential energy. Besides, we have demonstrated how a nonholonomic constraint behaves as a real potential energy setting the equilibrium point of the system, and how we can achieve asymptotic stability with this behavior. Furthermore, we have experimentally

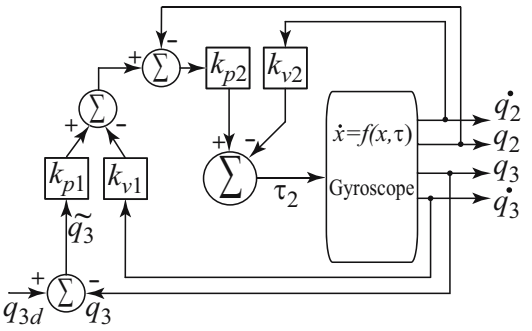

Fig. 4. Block diagram of the cascade PD-PD controller (90) applied to the gyroscope to compare it with the IDA-PBC (76).

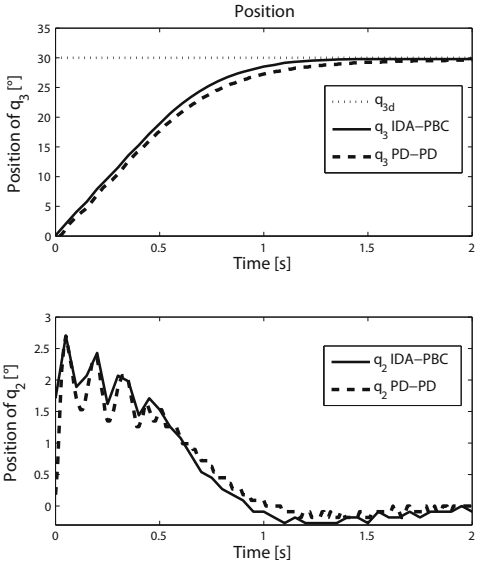

Fig. 5. Time evolution of q_3 and q_2 utilizing the IDA-PBC (76) in comparison with the cascade PD-PD controller (90).

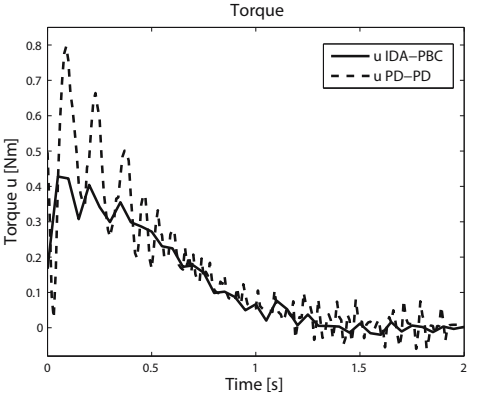

Fig. 6. Input control supplied from the IDA-PBC (76) in comparison with the torque of the cascade PD-PD controller (90).

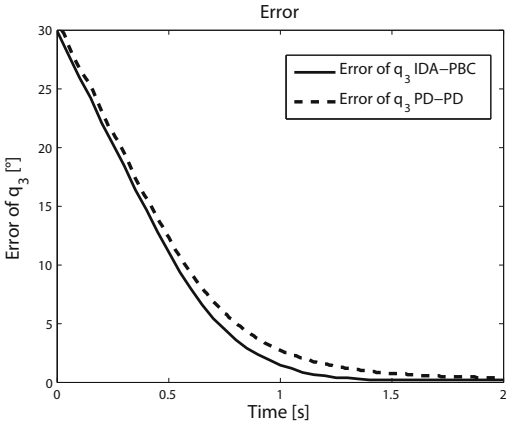

Fig. 7. Position error, $\tilde{q}_3 = q_{3d} - q_3$ utilizing the IDA-PBC (76) and the cascade PD-PD controller (90).

evaluated the performance of IDA-PBC versus a cascade PD-PD controller, showing the advantages of the proposed controller illustrated by faster responses and smaller errors.

7.1. Final remarks.

Remark 2. (*Original achievements*) In this paper we propose, as an original achievement, the design and practical implementation of IDA-PBC in a system having no potential energy. Furthermore, we propose an unconventional way to prove asymptotic stability, since without the help of a nonholonomic constraint neither the desired potential function, nor the desired Hamiltonian is positive definite. We prove that the nonholonomic constraint isolates one critical point of the desired Hamiltonian function, among many others, taking this function to be positive definite. Next, the direct Lyapunov method can be used, and then, LaSalle's theorem can lead us to asymptotic stability of the equilibrium point.

Remark 3. (*Potential practical implementation of results*) The knowledge resulting from this paper can be extended to others systems having no potential energy function and nonholonomic constraints.

Acknowledgment

This work was partially supported by TecNM, the CONACYT grant no. 134534 and the CONACYT grant no. 166636.

References

Acosta, J., Ortega, R., Astolfi, A. and Mahindrakar, A. (2005). Interconnection and damping assignment passivity-based control of mechanical systems with underactuation degree one, *IEEE Transactions on Automatic Control* **50**(12): 1936–1955.

Aguilar-Ibanez, C. (2016). Stabilization of the PVTOL aircraft based on a sliding mode and a saturation function, *International Journal of Robust and Nonlinear Control* **27**(5): 843–859.

Antonio-Cruz, M., Hernandez-Guzman, V.M. and Silva-Ortigoza, R. (2018). Limit cycle elimination in

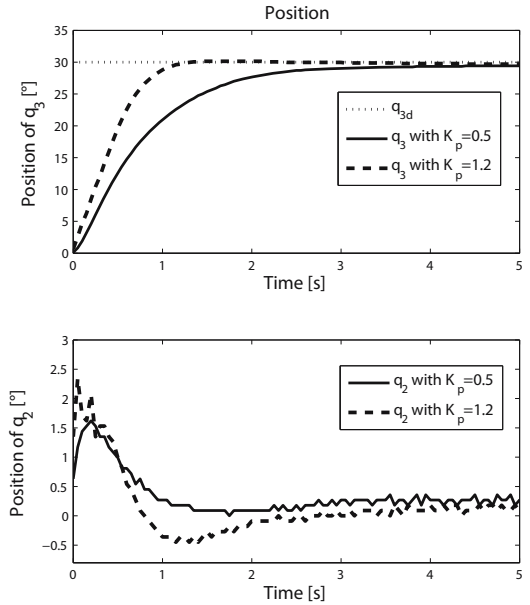

Fig. 8. Time evolution of q_3 and q_2 utilizing the IDA-PBC (76) for different values of K_p.

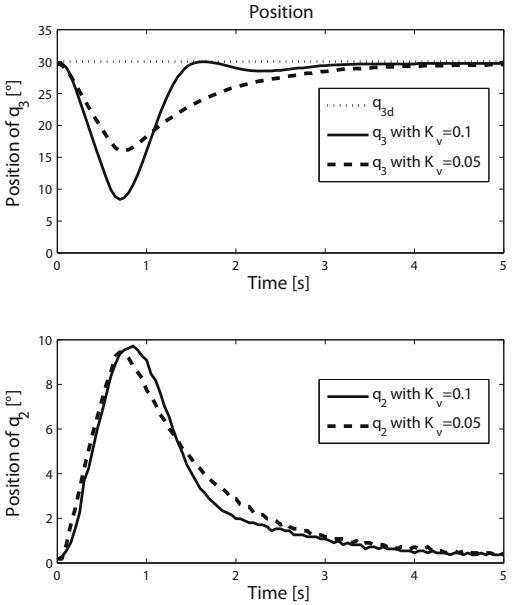

Fig. 9. Time evolution of q_3 and q_2 utilizing the IDA-PBC (76) rejecting disturbances with different values of K_v.

inverted pendulums: Furuta pendulum and pendubot, *IEEE Access* **6**: 30317–30332.

Bloch, A.M. (2003). *Nonholonomic Mechanics and Control*, Springer-Verlag, New York, NY.

Bloch, A.M., Reyhanoglu, M. and McClamroch, N.H. (1992). Control and stabilization of nonholonomic dynamic systems, *IEEE Transactions on Automatic Control* **37**(11): 1746–1757.

Cannon, R.H. (1967). *Dynamics of Physical Systems*, McGraw-Hill, New York, NY.

Chang, D. (2014). On the method of interconnection and damping assignment passivity-based control for the stabilization of mechanical systems, *Regular and Chaotic Dynamics* **19**(5): 556–575.

Chin, C.S., Lau, M.W.S., Low, E. and Seet, G.G.L. (2006). A robust controller design method and stability analysis of an underactuated underwater vehicle, *International Journal of Applied Mathematics and Computer Science* **16**(3): 345–356.

Donaire, A., Mehra, R., Ortega, R., Satpute, S., Romero, J.G., Kazi, F. and Singh, N.M. (2015). Shaping the energy of mechanical systems without solving partial differential equations, *American Control Conference, Chicago, IL, USA*, pp. 1351–1356.

Donaire, A., Romero, J.G., Ortega, R., Siciliano, B. and Crespo, M. (2016). Robust IDA-PBC for underactuated mechanical systems subject to matched disturbances, *International Journal of Robust and Nonlinear Control* **27**(6): 1000–1016.

Fantoni, I. and Lozano, R. (2002). *Non-linear Control for Underactuated Mechanical Systems*, Advances in Pattern Recognition, Springer, London.

Ferraz-Mello, S. (2007). *Canonical Perturbation Theories*, 1st Edn., Springer-Verlag, New York, NY.

Fulford, G., Forrester, P. and Jones, A. (1997). *Modelling with Differential and Difference Equations*, Australian Mathematical Society Lecture Series, Cambridge University Press, Cambridge.

Gómez-Estern, F. and van der Schaft, A. (2004). Physical damping in IDA-PBC controlled underactuated mechanical systems, *European Journal of Control* **10**(5): 451–468.

Greenwood, D.T. (1977). *Classical Dynamics*, Dover, New York, NY.

Jiang, Z.P. (2010). Controlling underactuated mechanical systems: A review and open problems, *in* J. Lévine and P. Müllhaupt (Eds.), *Advances in the Theory of Control, Signals and Systems with Physical Modeling*, Lecture Notes in Control and Information Sciences, Vol. 407, Springer, Berlin, pp. 77–88.

Kang, W., Xiao, M. and Borges, C. (2003). *New Trends in Nonlinear Dynamics and Control, and their Applications*, 1st Edn., Springer-Verlag, Heidelberg/Berlin.

Kelly, R., Santibánez, V. and Loría, A. (2005). *Control of Robot Manipulators in Joint Space*, 1st Edn., Springer-Verlag, London.

Kotyczka, P. and Lohmann, B. (2009). Parametrization of IDA-PBC by assignment of local linear dynamics, *Proceedings of the European Control Conference, Budapest, Hungary*, pp. 4721–4726.

Kozlov, V.V. (1996). *Symmetries, Topology and Resonances in Hamiltonian Mechanics*, 1st Edn., Springer-Verlag, Heidelberg/Berlin.

Layek, G.C. (2015). *An Introduction to Dynamical Systems and Chaos*, 1st Edn., Springer, New Delhi.

Liu, Y. (2018). Control of a class of multibody underactuated mechanical systems with discontinuous friction using sliding-mode, *Transactions of the Institute of Measurement and Control* **40**(2): 514–527.

Liu, Y. and Yu, H. (2013). A survey of underactuated mechanical systems, *IET Control Theory and Applications* **7**(7): 921–931.

Mahindrakar, A.D., Astolfi, A., Ortega, R. and Viola, G. (2006). Further constructive results on interconnection and damping assignment control of mechanical systems: The acrobot example, *International Journal of Robust and Nonlinear Control* **16**(14): 671–685.

Moreno-Valenzuela, J. and Aguilar-Avelar, C. (2018). *Motion Control of Underactuated Mechanical Systems*, 1st Edn., Springer International Publishing, Cham.

Nagata, W. and Namachchivaya, N.S. (2006). *Bifurcation Theory and Spatio-Temporal Pattern Formation*, Fields Institute Communications, Ontario.

Ortega, R., Spong, M., Gómez-Estern, F. and Blankeinstein, G. (2002). Stabilization of a class of underactuated mechanical systems via interconnection and damping assignment, *IEEE Transactions on Automatic Control* **47**(8): 1213–1233.

Ostrowski, J.P. and Burdick, J.W. (1997). Controllability for mechanical systems with symmetries and constraints, *Applied Mathematics and Computer Science* **7**(2): 305–331.

Parks, R. (1999). Manual for model 750 control moment gyroscope, *Technical document*, Educational Control Products, Bell Canyon, CA, `http://maecourses.ucsd.edu/ugcl/download/manuals/gyroscope.pdf`.

Quanser (2009). Specialty plant: 3 DOF gyroscope. User manual, *Document Number 806, Revision 1.0*, `https://www.quanser.com/products/3-dof-gyroscope`.

Rana, N. and Joag, P. (1991). *Classical Mechanics*, Tata McGraw-Hill, New Delhi.

Reyhanoglu, M. and van de Loo, J. (2006a). Rest-to-rest maneuvering of a nonholonomic control moment gyroscope, *IEEE International Symposium on Industrial Electronics, Montreal, Canada*, pp. 160–165.

Reyhanoglu, M. and van de Loo, J. (2006b). State feedback tracking of a nonholonomic control moment gyroscope, *Proceedings of the 45th IEEE Conference on Decision and Control, San Diego, CA, USA*, pp. 6156–6161.

Romero, J.G., Donaire, A., Ortega, R. and Borja, P. (2017). Global stabilisation of underactuated mechanical systems via PID passivity-based control, *IFAC PapersOnLine* **50**(1): 9577–9582.

Sabattini, L., Secchi, C. and Fantuzzi, C. (2017). Collision avoidance for multiple Lagrangian dynamical systems with gyroscopic forces, *International Journal of Advanced Robotic Systems* **1**(15): 1–15.

Sandoval, J., Kelly, R. and Santibanez, V. (2011). Interconnection and damping assignment passivity-based control of a class of underactuated mechanical systems with dynamic friction, *International Journal of Robust and Nonlinear Control* **21**(7): 738–751.

Sandoval, J., Ortega, R. and Kelly, R. (2008). Interconnection and damping assignment passivity-based control of the pendubot, *Proceedings of the 17th IFAC World Congress, Seoul, Korea*, pp. 7700–7704.

Santibanez, V., Kelly, R. and Llama, M.A. (2004). Global asymptotic stability of a tracking sectorial fuzzy controller for robot manipulators, *IEEE Transactions on Systems, Man, and Cybernetics B: Cybernetics* **34**(1): 710–718.

Seifried, R. (2014). *Dynamics of Underactuated Multibody Systems: Modeling, Control and Optimal Design (Solid Mechanics and Its Applications)*, Springer, Cham.

Seyranian, A., Stoustrup, J. and Kliem, W. (1995). On gyroscopic stabilization, *Journal of Applied Mathematics and Physics* **46**(2): 255–267.

She, J., Zhang, A., Lai, X. and Wu, M. (2012). Global stabilization of 2-DOF underactuated mechanical systems: An equivalent-input-disturbance approach, *Nonlinear Dynamics* **69**(1–2): 495–509.

Wichlund, K.Y., Sordalen, O.J. and Egeland, O. (1995). Control of vehicles with second-order nonholonomic constraints: Underactuated vehicles, *Proceedings of the 3rd European Control Conference, Rome, Italy*, pp. 3086–3091.

Gustavo Cordero was born in Lerdo, Durango, México, in 1984. He received the BE degree in electronic engineering and the MSc degree in mechatronics and control from the Laguna Institute of Technology, Mexico, in 2005 and 2013, respectively. He is currently a PhD student at the Laguna Institute of Technology. His research interests include robot control, passivity-based control, underactuated mechanisms, and Lyapunov and LaSalle stabilities.

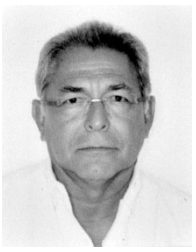

Víctor Santibáñez received the BE and MSc degrees in electronic engineering from the Laguna Institute of Technology, Torreón, Coahuila, México, and the PhD degree from CICESE, México, in 1977, 1984, and 1997, respectively. He has coauthored two books on robot control: *Control of Robot Manipulators* (Prentice Hall, 2003) and *Control of Robot Manipulators in Joint Space* (Springer, 2005). His research interests cover robot control, nonlinear systems control, fuzzy control and adaptive control.

Alejandro Dzul (S'99–M'03) was born in Gómez Palacio, México, in 1971. He received the BS degree in electronic engineering and the MS degree in electrical engineering, both from Instituto Tecnológico de La Laguna, México, in 1993 and 1997, respectively, and the PhD degree in automatic control from Université de Technologie de Compiégne, France, in 2002. Dr. Dzul has been a research professor with the Electrical and Electronic Engineering Department at Instituto Tecnologico de La Laguna since 2003. His current research interests are in the areas of nonlinear dynamics and control, and real-time control with applications to aerial vehicles.

Jesús Sandoval was born in Mazatlán, Mexico, in 1971. He received the BS degree in electrical engineering from the Culiacán Institute of Technology, Mexico, the MS degree in electrical engineering from the Laguna Institute of Technology, Mexico, and the DSc degree in automatic control from Baja California University, Mexico, in 1993, 1999 and 2010, respectively. He is a professor at the La Paz Institute of Technology, Mexico. His research interest include automatic control and mechatronics.

Appendix A

This appendix is devoted to obtaining the kinetic and potential energies of Quanser's gyroscope in order to obtain the dynamic model of Section 3. Figure A1 is a schematic representation of Quanser's 4-DOF gyroscope (it can be viewed as a rotating disc which has 3 DOFs). The selected configuration to work in the present paper has a rectangular frame A blocked, and the DC motor associated with it is no longer actuated implying a reduction by 1-DOF, converting our device into a 3-DOF gyroscope. The global $X_0Y_0Z_0$ axes are fixed to the ground, $X_IY_IZ_I$ with $I \in \{B, C, D\}$ are fixed to the rotating bodies, and all of them have the same origin. The q_3 position is associated with the rotation of the body B around the $Z_0 = Z_B$ axis and can be measured by the angle formed between the Y_0 and Y_B axes, as shown in Fig. A2(a). The q_2 position is associated with the rotation of the body C around the $Y_B = Y_C$ axis and can be measured by the angle formed between the Z_B and Z_C axes, as shown in Fig. A2(b). Finally, the position of the disc D is represented by the angle q_1 associated with the rotation around the $X_C = X_D$ axis and can be measured by the angle formed between the Y_C and Y_D axes, as shown in Fig. A2(c). As mentioned before, the frame A is fixed such that the associated angle q_4 measured with respect to the X_0 axis and its derivatives are set to zero, i.e, $q_4 = \dot{q}_4 = \ddot{q}_4 = 0$ (for this reason it is not shown in Fig. A1).

We use rotation matrices in $Z_0 = Z_B$, $Y_B = Y_C$ and $X_C = X_D$ axes to help us obtain the angular velocity of

each body. Thus

$$R_B^0 = \begin{bmatrix} C_3 & -S_3 & 0 \\ S_3 & C_3 & 0 \\ 0 & 0 & 1 \end{bmatrix}, \tag{A1}$$

$$R_C^B = \begin{bmatrix} C_2 & 0 & S_2 \\ 0 & 1 & 0 \\ -S_2 & 0 & C_2 \end{bmatrix}, \tag{A2}$$

$$R_D^C = \begin{bmatrix} 1 & 0 & 0 \\ 0 & C_1 & -S_1 \\ 0 & S_1 & C_1 \end{bmatrix}, \tag{A3}$$

where $C_i = \cos(q_i)$ and $S_i = \sin(q_i)$ with $i \in \{1, 2, 3\}$.

Assume that, in general, the angular velocity of the body I with respect to the frame of the body J ($I, J \in \{B, C, D\}$) is represented by the vector $\boldsymbol{\omega}_I^J$. We have

$$\boldsymbol{\omega}_B^0 = \begin{bmatrix} 0 \\ 0 \\ \omega_3 \end{bmatrix}, \tag{A4}$$

$$\boldsymbol{\omega}_C^B = \begin{bmatrix} 0 \\ \omega_2 \\ 0 \end{bmatrix}, \tag{A5}$$

$$\boldsymbol{\omega}_D^C = \begin{bmatrix} \omega_1 \\ 0 \\ 0 \end{bmatrix}, \tag{A6}$$

where $\omega_i = \dot{q}_i$ with $i = 1, 2, 3$. Then, the angular velocity of the bodies B, C and D, with respect to their own frame, is obtained as follows:

$$\boldsymbol{\omega}_B^B = R_0^B \boldsymbol{\omega}_B^0 = (R_B^0)^T \boldsymbol{\omega}_B^0, \tag{A7}$$

$$\boldsymbol{\omega}_C^C = (R_C^B)^T (\boldsymbol{\omega}_B^B + \boldsymbol{\omega}_C^B), \tag{A8}$$

$$\boldsymbol{\omega}_D^D = (R_D^C)^T (\boldsymbol{\omega}_C^C + \boldsymbol{\omega}_D^C). \tag{A9}$$

By substituting the rotation matrices R_B^0, R_C^B, R_D^C, given in (A1)–(A3), and the angular velocity vectors $\boldsymbol{\omega}_B^0$, $\boldsymbol{\omega}_C^B$ and $\boldsymbol{\omega}_D^C$, given in (A4)–(A6) into Eqns. (A7)–(A9)

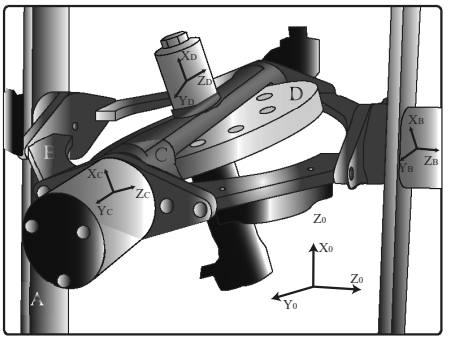

Fig. A1. Schematic representation of the gyroscope in an arbitrary configuration.

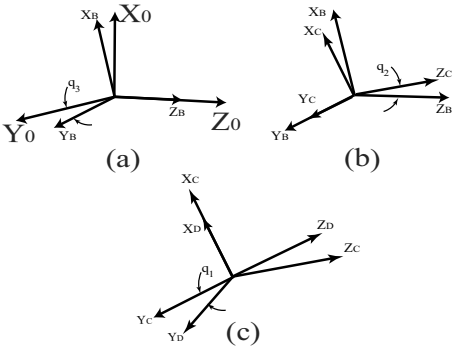

Fig. A2. Relative movement of each frame of the gyroscope.

and, making some basic operations, we get the following angular velocities:

$$\boldsymbol{\omega}_B^B = \begin{bmatrix} 0 \\ 0 \\ \dot{q}_3 \end{bmatrix}, \tag{A10}$$

$$\boldsymbol{\omega}_C^C = \begin{bmatrix} -S_2\dot{q}_3 \\ \dot{q}_2 \\ C_2\dot{q}_3 \end{bmatrix}, \tag{A11}$$

$$\boldsymbol{\omega}_D^D = \begin{bmatrix} \dot{q}_1 - S_2\dot{q}_3 \\ \dot{q}_2 \\ C_2\dot{q}_3 \end{bmatrix}, \tag{A12}$$

taking into account that the expression of the angular velocity $\boldsymbol{\omega}_D^D$ has been simplified in terms of q_1 due to the axial symmetry of body D and by recognizing that only angular velocity of the disc ω_1, and not its position q_1, is needed in the dynamics and control study of the system, as stated by Parks (1999).

The kinetic energy of each body of the gyroscope is obtained from the equation $\mathcal{K}(q(t), \dot{q}(t)) = \frac{1}{2}\sum_{I=A}^{D} \boldsymbol{\omega}_I^{I^T} \mathbf{I}_I \boldsymbol{\omega}_I^I$, where $\mathbf{I}_I$ is the moment of inertia matrix of the body I referred to the frame of the same body. Only moments of inertia are considered while products of inertia are set to zero due to the geometry of the bodies. (Note that there is no translation motion, and, in consequence, the term $\frac{1}{2}m_I\mathbf{v}_I^T\mathbf{v}_I$ is suppressed from the kinetic energy equation, where $\mathbf{v}_I$ denotes the translational velocity.)

The kinetic energy of body D can be expressed as follows:

$$\mathcal{K}_D = \frac{1}{2}I_{Dxx}\dot{q}_1^2 + \frac{1}{2}I_{Dyy}\dot{q}_2^2 + \frac{1}{2}I_{Dzz}\dot{q}_3^2 - I_{Dxx}S_2\dot{q}_1\dot{q}_3 + \frac{1}{2}(I_{Dxx} - I_{Dzz})S_2^2\dot{q}_3^2. \tag{A13}$$

Furthermore, the kinetic energy of body C is

$$\mathcal{K}_C = \frac{1}{2}(I_{Cxx} - I_{Czz})S_2^2\dot{q}_3^2 + \frac{1}{2}I_{Cyy}\dot{q}_2^2 + \frac{1}{2}I_{Czz}\dot{q}_3^2. \tag{A14}$$

In addition, the kinetic energy of body B takes the form

$$\mathcal{K}_B = \frac{1}{2} I_{Bzz} \dot{q}_3^2. \tag{A15}$$

Finally, the total kinetic energy ($\mathcal{K} = \mathcal{K}_B + \mathcal{K}_C + \mathcal{K}_D$) with some factorizations is

$$\begin{aligned}\mathcal{K} = {} & \frac{1}{2} I_{Dxx} \dot{q}_1^2 + \frac{1}{2} J_3 \dot{q}_2^2 \\ & - I_{Dxx} S_2 \dot{q}_1 \dot{q}_3 + \frac{1}{2}(J_2 + J_1 S_2^2)\dot{q}_3^2,\end{aligned} \tag{A16}$$

where $J_1 = I_{Cxx} - I_{Czz} - I_{Dzz} + I_{Dxx}$, $J_2 = I_{Bzz} + I_{Czz} + I_{Dzz}$ and $J_3 = I_{Cyy} + I_{Dyy}$, with I_{Bzz} being the moment of inertia of the body B around the Z_B axis, I_{Cxx}, I_{Cyy} and I_{Czz} the moments of inertia of the body C around the X_C, Y_C and Z_C axes, respectively, and I_{Dxx}, I_{Dyy} and I_{Dzz} the moments of inertia of the body D around the X_D, Y_D and Z_D axes, respectively.

Since the center of mass is fixed and it is the same center for all associated frames, and due to the symmetric property of the bodies, the potential energy function yields

$$V(q) = 0. \tag{A17}$$

Appendix B

In this appendix, we prove the identity between Eqns. (23) and (49). First, consider the generalized potential energy function introduced in Definition 5, i.e., the sum of the ordinary potential energy function and a gyroscopic term that is linear in $\dot{q}$,

$$W(q, \dot{q}) = V(q) + \varphi^\top(q)\dot{q}. \tag{B1}$$

Now, we write Eqn. (B1) in terms of (q, p), by calling (22) and solving for $\dot{q}$, we have

$$\dot{q} = M^{-1} p + M^{-1} \frac{\partial W(q, \dot{q})}{\partial \dot{q}}; \tag{B2}$$

then, by substituting (B2) into (B1), we have

$$W(q, p) = V + \varphi^\top M^{-1} p + \varphi^\top M^{-1} \frac{\partial W(q, \dot{q})}{\partial \dot{q}}. \tag{B3}$$

Besides, if we get the derivative of (B1) with respect to $\dot{q}$, we obtain

$$\frac{\partial W}{\partial \dot{q}} = \frac{\partial}{\partial \dot{q}}[V(q) + \varphi^\top(q)\dot{q}] = \frac{\partial[\varphi \dot{q}]}{\partial \dot{q}} = \varphi. \tag{B4}$$

By substituting (B4) into (B3), we get

$$\begin{aligned}W(q, p) = {} & V + \left(\frac{\partial W(q, \dot{q})}{\partial \dot{q}}\right)^\top M^{-1} p \\ & + \left(\frac{\partial W(q, \dot{q})}{\partial \dot{q}}\right)^\top M^{-1} \frac{\partial W(q, \dot{q})}{\partial \dot{q}}.\end{aligned} \tag{B5}$$

Now, we are ready to begin the demonstration. By substituting (24) into (23), we obtain

$$\begin{aligned}H = {} & \frac{1}{2} p^\top M^{-1} p + W(q, p) \\ & - \frac{1}{2}\left(\frac{\partial W(q, \dot{q})}{\partial \dot{q}}\right)^\top M^{-1} \frac{\partial W(q, \dot{q})}{\partial \dot{q}};\end{aligned} \tag{B6}$$

if we substitute (B5) in (B6), we arrive at

$$\begin{aligned}H = {} & \frac{1}{2} p^\top M^{-1} p + \left(\frac{\partial W}{\partial \dot{q}}\right)^\top M^{-1} p \\ & + \frac{1}{2}\left(\frac{\partial W}{\partial \dot{q}}\right)^\top M^{-1} \frac{\partial W}{\partial \dot{q}} + V.\end{aligned} \tag{B7}$$

Without the function V, the other terms in (B7) form a perfect-square trinomial, and consequently Eqn. (B7) can be reduced to

$$H = \frac{1}{2}\left[p + \frac{\partial W}{\partial \dot{q}}\right]^\top M^{-1}\left[p + \frac{\partial W}{\partial \dot{q}}\right] + V. \tag{B8}$$

Therefore, the identity between Eqns. (23) and (49) is demonstrated.

Appendix C

The first order autonomous nonlinear differential equation

$$k_4 \frac{\mathrm{d}q_2(t)}{\mathrm{d}t} \equiv k_3 P_1[\sin(q_2(t)) - \sin(q_2(0))], \tag{C1}$$

previously presented in (86), has the form

$$\frac{\mathrm{d}x}{\mathrm{d}t} = f(x), \tag{C2}$$

which is separable as

$$t + \mathrm{IC} = \int \frac{\mathrm{d}x}{f(x)}, \tag{C3}$$

where $x = q_2$, $f(x) = (k_3/k_4)P_1[\sin(q_2(t)) - \sin(q_2(0))]$ and IC as an integration constant. Stationary solutions[2] of (C2) are found when $\mathrm{d}x(t)/\mathrm{d}t = 0$, i.e., $f(x) = 0$ (Fulford *et al.*, 1997). For (C1),

$$\begin{aligned}f(x) &= f(q_2) \\ &= \frac{k_3}{k_4} P_1[\sin(q_2(t)) - \sin(q_2(0))] = 0,\end{aligned} \tag{C4}$$

which yields

$$q_2(t) = q_2(0), \tag{C5}$$

[2]Stationary solutions or steady state solutions are time-independent constant solutions (Fulford *et al.*, 1997).

as stated in (87). For nonstationary solutions of (C2), we solve the differential equation (C1) as proposed in (C3), obtaining

$$t + \text{IC} = \frac{k_4}{k_3 P_1} \int \frac{\mathrm{d}q_2(t)}{(\sin(q_2(t)) - \sin(q_2(0)))}. \quad \text{(C6)}$$

By calculating the integral of (C6), we have

$$t + \text{IC} = \frac{2k_4}{k_3 P_1 \alpha} \arctan\left[\frac{1 - \sin(q_2(0)) \tan(\frac{q_2(t)}{2})}{\alpha}\right], \quad \text{(C7)}$$

where

$$\alpha = \sqrt{\sin^2(q_2(0)) - 1} = \cos(q_2(0))i, \quad \text{(C8)}$$

i being an imaginary number. The above expression (C7) does not have a real solution for $q_2(t)$, because α is not a real number for all $q_2(0) \neq n\pi/2$, where $n = \{\ldots, -3, -1, 1, 3, 5, \ldots\}$; moreover, when $q_2(0) = n\pi/2$, the right-hand-side term of (C7) is not defined due to $\alpha = 0$. Then, we conclude that (C5) is the unique real solution for (C1).

Received: 23 November 2017
Revised: 25 May 2018
Re-revised: 27 June 2018
Accepted: 15 July 2018